Growth Factors, Cytokines, Cell Cycle Molecules

Ultrasound-Microbubble-Mediated Gene Transfer of Inducible Smad7 Blocks Transforming Growth Factor-β Signaling and Fibrosis in Rat Remnant Kidney

Chun-Cheng Hou,*[†] Wansheng Wang,[†]
Xiao R. Huang,[†] Ping Fu,[†] Tso-Hsiao Chen,*
David Sheikh-Hamad,[†] and Hui Y. Lan[†]

From the Department of Medicine, Municipal Wan-Fang
Hospital, Taipei Medical University, Taipei, Taiwan, Republic of
China; and the Department of Medicine-Nephrology,[†] Baylor
College of Medicine, Houston, Texas*

Transforming growth factor (TGF)-β1 has been shown to play a critical role in hypertensive nephropathy. We hypothesized that blocking TGF-β1 signaling could attenuate renal fibrosis in a rat model of remnant kidney disease. Groups of six rats were subjected to 5/6 nephrectomy and received renal arterial injection of a doxycycline-regulated Smad7 gene or control empty vector using an ultrasound-microbubble-mediated system. Smad7 transgene expression within the kidney was tightly controlled by the addition of doxycycline in the daily drinking water. All animals were euthanized at week 4 for renal functional and histological examination. Hypertension of equivalent magnitude (190 to 200 mmHg) developed in both Smad7- and empty vector-treated rats. However, treatment with Smad7 substantially inhibited Smad2/3 activation and prevented progressive renal injury by inhibiting the rise of 24-hour proteinuria (*P* < 0.001) and serum creatinine (*P* < 0.001), preserving creatinine clearance (*P* < 0.05), and attenuating renal fibrosis and vascular sclerosis such as collagen I and III expression (*P* < 0.01) and myofibroblast accumulation (*P* < 0.001). In conclusion, TGF-β/Smad signaling plays a critical role in renal fibrosis in a rat remnant kidney model. The ability of Smad7 to block Smad2/3 activation and attenuate renal and vascular sclerosis demonstrates that ultrasound-mediated Smad7 gene therapy may be a useful therapeutic strategy for the prevention of renal fibrosis in association with hypertension. *(Am J Pathol 2005, 166:761–771)*

Renal fibrosis is a final common pathway to end-stage renal disease. Recent studies have shown that hypertensive nephropathy is a major leading cause of end-stage renal disease and the renin-angiotensin system plays a pivotal role in the development of progressive renal injury.[1,2] Clinical trials have shown that blocking the effects of angiotensin II (Ang II) with angiotensin-converting enzyme inhibitors and angiotensin-receptor blockers can prevent or slow the progression of kidney damage in patients with diabetes and hypertension.[1–3]

The mechanism of renal fibrosis associated with hypertension involves stimulation of transforming growth factor (TGF)-β by Ang II.[4–6] According to this view, Ang II and TGF-β are critical mediators of renal fibrosis.[4–6] Indeed, Ang II can induce extracellular matrix (ECM) expression by glomerular mesangial cells,[7,8] tubular epithelial cells,[9,10] and vascular smooth cells[11] through a TGF-β-dependent mechanism. Attenuation of progressive renal injury in rat remnant kidney model by use of Ang II receptor blockade has been shown to involve inhibition of renal TGF-β expression.[12–14] A similar result is also evident in human hypertensive/diabetic nephropathy in which inhibition of the renin-angiotensin system with angiotensin-converting enzyme inhibitors or angiotensin-receptor blockers delays disease progression in association with reduction of urinary TGF-β excretion.[15,16] All these studies indicate that Ang II may mediate renal scarring through TGF-β stimulation.

TGF-β1 is the putative key mediator of fibrosis in both experimental and human chronic kidney disease.[4–6] This is supported by the findings that overexpression of the

TGF-β1 gene leads to renal fibrosis,[17] whereas blockade of TGF-β with anti-sense oligonucleotides, decorin, or a neutralizing antibody attenuates renal scaring.[18–20] Of note, TGF-β induces ECM-related gene expression through activation of Smad2/3.[21] On binding to its receptors, TGF-β activates receptor-associated Smads (Smad2/3). Once activated, Smad2 and Smad3 associate with the common partner Smad4 and translocate to the nucleus, where Smad protein complexes participate in transcriptional control of target genes. In addition, activation of TGF-β signaling can also result in the expression of inhibitory Smads, which include Smad6 and Smad7. These inhibitory Smads decrease Smad2/3 phosphorylation by blocking their access to TGF-β receptors or causing degradation of TGF-β receptors via a negative feedback mechanism.[22] Increasing evidence has shown that TGF-β/Smad signaling plays a critical role in renal fibrosis.[23–26] This is supported by studies showing that Smad2/3 is activated in diabetic nephropathy[27,28] and that overexpression of Smad7 by gene transfer can inhibit TGF-β-induced Smad2/3 activation and ECM production *in vitro*[29,30] and in the obstructive rat kidney model.[31,32] We, thus, hypothesized that blockade of the TGF-β signaling pathway by gene transfer of an inducible Smad7 gene may be able to attenuate progressive renal injury in the 5/6 nephrectomized rat model and may represent a specific therapeutic strategy to block renal fibrosis in kidney diseases with hypertension. Gene transfer was achieved with the ultrasound-microbubble technique and Smad7 transgene expression was tightly regulated by the addition of doxycycline in the drinking water. The results showed that overexpression of Smad7 attenuated renal fibrosis and prevented renal function impairment in this hypertensive kidney disease model.

Materials and Methods

Ultrasound-Mediated Gene Transfer of Inducible Smad7 Gene-Loaded Microbubbles into the Kidney

To control Smad7 transgene expression within the kidney at the therapeutic levels without undesirable effects, a doxycycline-regulated Smad7-expressing plasmid was used.[31] Briefly, a mouse Smad7 cDNA with a flag tag (m2) at its NH2 terminus in pcDNA3 (gift from Dr. P. ten Dijke, The Netherlands Cancer Institute, Amsterdam, The Netherlands) was subcloned into a tetracycline-inducible vector, pTRE (Clontech, Palo Alto, CA), to obtain pTRE-m2Smad7. An improved pTet-on vector (Clontech), pEF-purop-Tet-on, was generously provided by G. Vario (Cerylid, Melbourne, Australia). All plasmids were prepared using the EndoFree plasmid kit (Qiagen Inc., Valencia, CA) as per the manufacturer's instructions. To achieve doxycycline-inducible Smad7 transgene expression, the ultrasound-microbubble-mediated system was applied as previously described.[31] Briefly, after mixing pTRE-m2Smad7 and pEFpurop-Tet-on with albumin perflutren-filled microbubbles (Optison; Mallinckrodt, St. Louis, MO) at a ratio of 1:1 (v/v), the mixed solution

containing 15 μg of designated plasmids in 0.3 ml was injected into the left remnant kidney via the renal artery while temporarily clipping off proximal portions of the renal artery and vein (less than 5 minutes). Immediately after injection, the ultrasound transducer (Ultax UX-301; Celcom Medico Inc., Fukuoka, Japan) was directly applied to one side of the kidney and a continuous-wave output of 1 MHz at 5% power output was applied for a total of 60 seconds with a 30-second interval. Ultrasound treatment was applied to the other side of the kidney using the same procedure.

Animal Model and Protocol

Male Sprague-Dawley rats at 6 weeks of age, weighing 220 to 250 g, were obtained from Harlan (Indianapolis, IN). Progressive renal disease model with hypertension was induced by 5/6 subtotal nephrectomy as previously described.[33] Briefly, 12 animals underwent subtotal nephrectomy involving right subcapsular nephrectomy and infarction of approximately two-thirds of the left kidney by ligation of the posterior and one or two anterior extrarenal branches of the renal artery. Immediately after the surgery, rats were randomly assigned into groups of six animals and received either Smad7 or empty vectors as previously described.[31] In the treatment group, six rats were injected with a mixture (0.3 ml) of pTRE-m2Smad7 plus Tet-on plasmids plus Optison into the left kidney at a dose of 15 μg/kidney via the renal artery and treated with ultrasound as described above. Control animals received the same procedure, except for substitution of pTRE-m2Smad7 with empty vector. To induce Smad7 transgene expression, 1 ml of doxycycline (Sigma, St. Louis, MO) at a concentration of 200 μg/ml was administered into the peritoneal cavity immediately after ultrasound-microbubble gene transfer, followed by the addition of doxycycline in the daily drinking water (200 μg/ml) for 28 days as previously described.[31] For normal controls, six rats underwent a sham operation consisting of laparotomy and manipulation of the renal pedicles but without damage to the kidney. All rats were euthanized at day 28 after disease induction. Rat serum was collected at day 0 and weeks 2 and 4 for creatinine determination, and 24-hour urine samples were collected in metabolic cages at day 0 and weekly for the determination of urinary levels of protein and creatinine excretion. All procedures were performed in accordance with Institutional Guidelines for Animal Care.

Renal Function Assessment and Blood Pressure Measurement

Urinary protein concentrations were determined by the Bradford method, adapted to a microtiter plate assay. Coomassie reagent (USB, Cleveland, OH) was added to the diluted urine samples. After 10 minutes, the absorbance at 595-nm wavelength was read on ELX800 microplate reader (Bio-Tek Instruments, VT). The protein concentrations were calculated by reference to bovine serum albumin (Sigma) standards. Serum and urine cre-

atinine were analyzed using a creatinine kit (Sigma). Systolic blood pressure was recorded by tail plethysmography using the BP2000 blood pressure analysis system (Visitech Systems, Inc., Apex, NC) in conscious rats at baseline and every 2 weeks throughout the experimental time course.

Real-Time Polymerase Chain Reaction (PCR)

Total RNA was isolated from snap-frozen, noninfarcted kidney tissues using the RNAeasy isolation kit (Qiagen) according to the manufacturer's instructions. Real-time reverse transcriptase (RT)-PCR was performed as previously described.[34] Briefly, a real-time PCR was performed using Bio-Rad (Hercules, CA) iQ SYBR Green supermix with Opticon (MJ Research Inc., Waltham, MA), according to the manufacturer's instructions. One hundred μg of total RNA were reverse-transcribed and subjected to PCR as follows: 94°C for 2 minutes followed by 40 cycles at 94°C for 15 seconds, 58°C for 30 seconds, 72°C for 30 seconds, with final extension at 72°C for 10 minutes. The primers used in this study were: rat Smad7, forward 5′- CGCTGTACCTTC-CTCCGAT-3′, reverse 5′-ATGAAAGATGGCTGGAA-GAGGGTC-3′; α-smooth muscle actin (SMA), forward 5′-ACTGGGACGACATGGAAAAG-3′, reverse 5′-CATCTC-CAGAGTCCAGCACA-3′; collagen I, forward 5′-GAGCG-GAGAGTACTGGATCG-3′, reverse 5′-TACTCGAACGG-GAATCCATC-3′; and collagen III, forward 5′-TGGTC-CTCAGGGTGTAAAGG-3′, reverse 5′-GTCCAGCATCAC-CTTTTGGT-3′. All samples were subjected to RT-PCR for the housekeeping gene GAPDH, forward 5′-TGCTGAG-TATGTCGTGGAGTCTA-3′, reverse 5′-AGTGGGAGTT-GCTGTTGAAATC-3′ as an internal standard. Reaction specificity was confirmed by gel electrophoresis of products after real-time PCR and melting curve analysis. Ratios for Smad7/GAPDH, α-SMA/GAPDH, collagen I/GAPDH, and collagen III/GAPDH mRNA were calculated for each sample and expressed as the means ± SEM.

Western Blotting and Immunoprecipitation

Western blot analysis was used for detection of Smad7, α-SMA, and collagen type I and type III expression within the kidney, whereas immunoprecipitation was used for detection of phosphorylated Smad2/3 as previously described.[28,31] Snap-frozen, noninfarcted kidney tissues were lysed in 1 ml of 1% Nonidet P-40, 25 mmol/L Tris-HCl, 150 mmol/L NaCl, 10 mmol/L ethylenediaminetetraacetic acid, pH 8.0, containing protease inhibitor cocktail (P2714, at a final dilution of 1:50; Sigma) for 30 minutes on ice. Samples (20 μg) were centrifuged at 14,000 × g for 5 minutes to pellet cell debris, mixed with sodium dodecyl sulfate-polyacrylamide gel electrophoresis sample buffer, boiled for 5 minutes, electrophoresed on a 10% sodium dodecyl sulfate polyacrylamide gel, and electroblotted onto polyvinylidene difluoride nitrocellulose membrane (Amersham International, Buckinghamshire, UK). The membrane was blocked in Tris-buffered saline containing 5% bovine serum albumin and 0.02% Tween 20 and incubated for 1 hour with one of the fol-

lowing: mouse monoclonal antibodies (mAbs) to α-SMA (Sigma), goat polyclonal antibodies to Smad7 (Santa Cruz Biotechnology Inc., Santa Cruz, CA), goat anti-collagen I or anti-collagen III (Southern Biotech, Birmingham, AL). After washing, the membrane was incubated with peroxidase-conjugated goat anti-mouse IgG or rabbit anti-goat IgG in phosphate-buffered saline containing 1% normal goat serum and 1% fetal calf serum. Phosphorylated Smad2/3 was determined by immunoprecipitation with anti-Smad2/3 antibody followed by immunoblotting and detection with rabbit anti-phosphoserine antibody.[28,31] After washing, bands were detected using the ECL kit (Amersham) and signal was captured on X-ray film.

Histology and Immunohistochemistry

Renal tissues for histological examination were fixed in 10% formalin and 4-μm paraffin sections were stained with hematoxylin and eosin and periodic acid-Schiff (PAS). To detect activation of Smad2/3 and expression of Smad7, 4-μm paraffin sections were stained with rabbit polyclonal antibodies to p-Smad2/3 (Santa Cruz) and goat antibody to Smad7 (Santa Cruz), using a microwave-based antigen retrieval technique and a peroxidase anti-peroxidase method as previously described.[28,31] An irrelevant isotype rabbit or goat IgG was used for negative control. The degree of interstitial myofibroblast accumulation and collagen I and III expression were determined using microwave-based antigen retrieval method with anti-α-SMA mAb (Sigma) and anti-rat collagen I and III polyclonal antibodies (Southern Biotech). Sections were then developed with diaminobenzidine to produce a brown color and counterstained with hematoxylin.
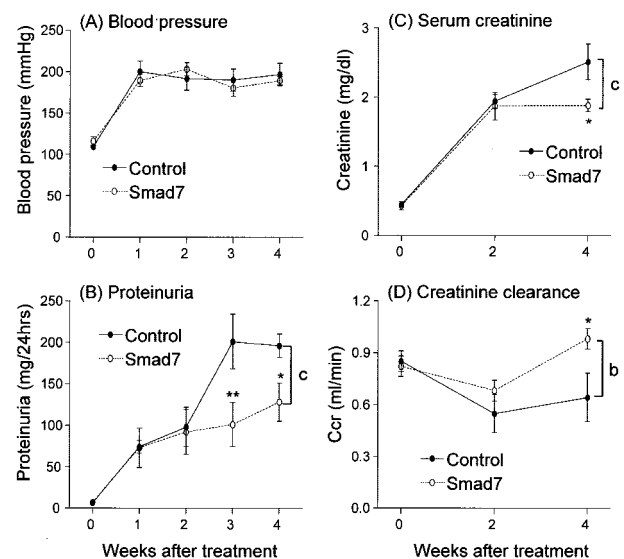

Figure 1. Effect of gene transfer with Smad7 on blood pressure and renal function in 5/6 nephrectomy in rats. **A:** Systolic blood pressure. **B:** Twenty-four-hour urinary protein excretion. **C:** Serum creatinine. **D:** Creatinine clearance. Data represent the means ± SEM for groups of six rats treated with either Smad7 or empty vector (comparison between Smad7- and empty vector-treated controls using analysis of variance: b, P < 0.01 and c, P < 0.001; and comparison between time-matched controls using t-test: *, P < 0.05 and **, P < 0.01).
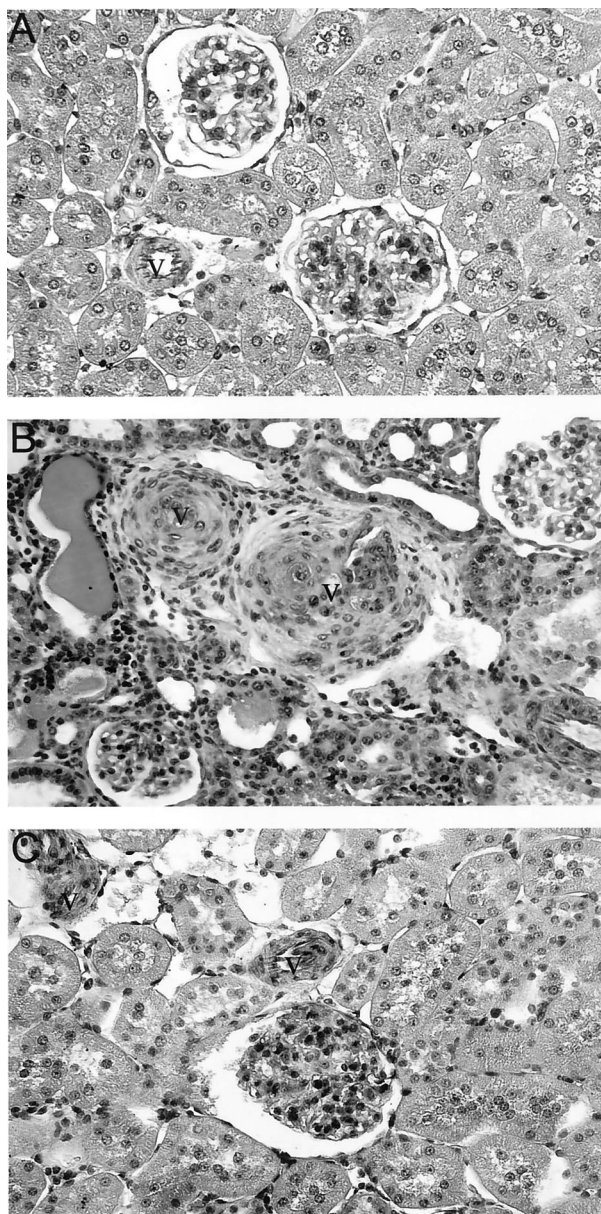
Figure 2. Effect of gene transfer with Smad7 on renal histological damage in 5/6 nephrectomy in rats. **A:** Normal sham-control, showing normal kidney histology. **B:** Diseased kidney from empty vector-treated controls exhibits severe tubulointerstitial fibrosis and vascular sclerosis (v). **C:** Diseased kidney from Smad7-treated rats shows that treatment with Smad7 prevents renal and vascular (v) damage. Kidney sections are stained with PAS. Original magnifications, ×200.

Quantitative Analyses

Smad2/3 activation was determined by the extent of its nuclear localization in stained tissue using anti-phosphorylated Smad2/3 antibody. The number of positive cells for activated Smad2/3 was counted in 20 consecutive glomeruli and expressed as cells/glomerular cross-section (gcs), whereas positive cells for activated Smad2/3 in the tubulointerstitium were counted under high-power fields (×40) by means of a 0.25-mm^2 graticule fitted in the eyepiece of the microscope, and expressed as cells per cm^2. Because Smad7 was widely expressed in the
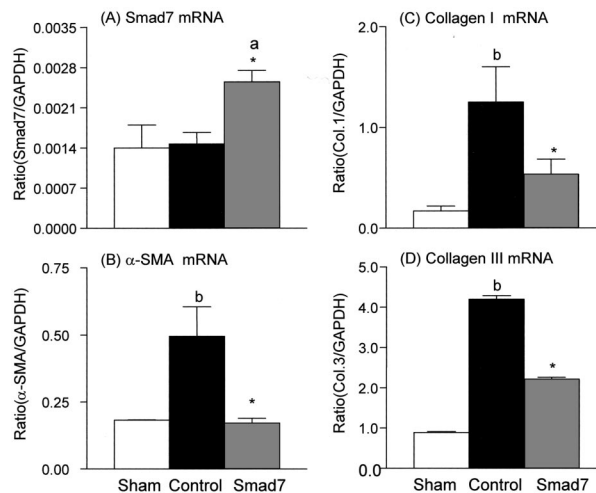

Figure 3. Real-time PCR reveals the inhibitory effect of Smad7 gene transfer on renal ECM mRNA expression. **A:** Smad7 mRNA. **B:** α-SMA mRNA. **C:** Collagen I mRNA. **D:** Collagen III mRNA. Each **bar** represents the means ± SEM for groups of six rats treated with Smad7 (**hatched bars**), empty vector (**filled bars**), or normal sham-control (**open bars**). *, $P < 0.05$ and **, $P < 0.01$, when compared against empty vector-treated controls; [a], $P < 0.05$ and [b], $P < 0.01$, when compared to normal sham-controls.

tubulointerstitium in both normal and diseased animals, semiquantitation of Smad7 expression in the tubulointerstitium was scored as follows: 0.5, weak; 1, mild; 2, moderate; 3, strong. The degree of glomerular Smad7 expression and accumulation of α-SMA and collagens type I and III in glomeruli and entire cortical tubulointerstitium (a cross-section of the kidney) were determined using quantitative Image Analysis System (Optima 6.5; Media Cybernetics, Silver Spring, MD). Briefly, the examined area of the glomerulus or the tubulointerstitium was outlined; positive staining patterns were identified, and the percent positive area in the examined glomerulus or
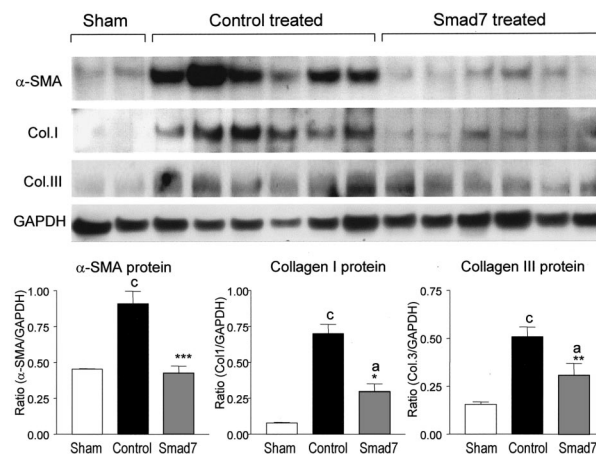

Figure 4. Western blot analysis shows the inhibitory effect of Smad7 gene transfer on renal ECM protein expression. Compared to normal sham-controls, expression of α-SMA, collagen type I, and collagen type III proteins is markedly increased in empty vector-treated animals, which is substantially inhibited by gene transfer with Smad7. Each **lane** represents one rat kidney and each **bar** represents semiquantitative data (mean ± SEM) for groups of six rats treated with Smad7 (**hatched bars**), empty vector (**filled bars**), or normal sham-control (**open bars**). *, $P < 0.05$ and **, $P < 0.01$, when compared to empty vector-treated controls; [b], $P < 0.01$ and [c], $P < 0.001$, when compared to the normal sham-control.

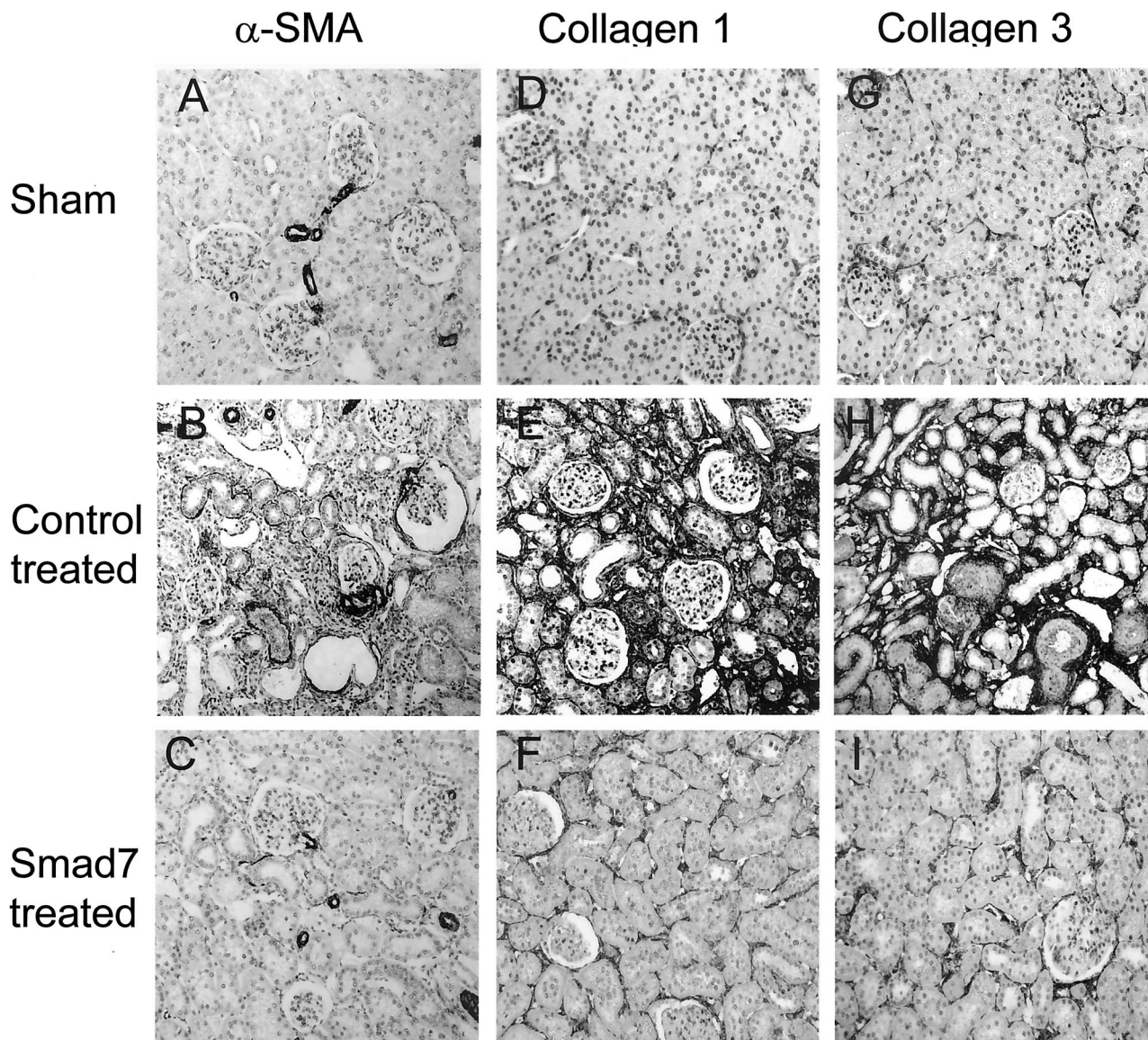α-SMA   Collagen 1   Collagen 3

Figure 5. Immunohistochemistry demonstrates that gene transfer with Smad7 inhibits renal α-SMA, collagen type I, and collagen type III accumulation within the kidney. **A–C:** α-SMA. **D–F:** Collagen type I. **G–I:** Collagen type III. The accumulation of α-SMA, collagen I, and collagen III in the tubulointerstitium is markedly increased in empty vector-treated animals (**B**, **E**, **H**), compared to normal sham-controls (**A**, **D**, **G**), which is substantially inhibited in 5/6 nephrectomized rats treated with Smad7 (**C**, **F**, **I**). Original magnifications, ×100.

tubulointerstitium was then measured. The spaces in Bowman's capsule and large arteries, including the arterial walls and periarterial areas were excluded from the study. Data were expressed as percent positive area examined. To investigate vascular Smad2/3 activation and vascular sclerosis, a point-counting technique was applied. Smad2/3-positive cells in arterial walls and immediate periarterial areas with or without the development of proliferative and sclerotic vasculopathy in the entire cortex were counted under 0.25-mm^2 graticule and expressed as cells per cm^2, whereas collagen matrix accumulation was measured using quantitative Image Analysis System as described above. The arterial lumen space was excluded from the study and the periarterial area was defined by the outline of tubular basement membrane surrounding the artery examined. Generally, 7 to 10 arteries in the entire cortex

were identified and examined. All analyses were performed in the same paraffin-block of renal tissue cross-sections that were far from the infracted areas (two to three low-power fields from the infracted tissues). All scoring was performed in a blinded manner on coded slides.

Statistical Analyses

Data obtained from this study are expressed as the means ± SEM. Statistical analyses were performed using GraphPad Prism 3.0 (GraphPad Software, Inc., San Diego, CA). Differences in blood pressure, proteinuria, serum creatinine, and creatinine clearance at different time points (weeks 0 to 4) within and between the groups, and differences of Smad2/3 activation, Smad7 expression, and
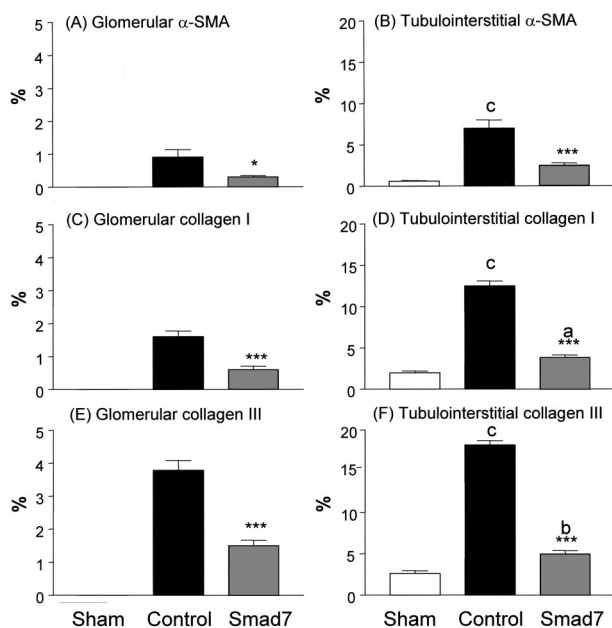
Figure 6. Semiquantitative analysis of the therapeutic effect of Smad7 on renal α-SMA, collagen I, and collagen III accumulation within the glomerulus and tubulointerstitium using the Quantitative Image System. **A, B:** Percentage of glomerular and tubulointerstitial α-SMA accumulation. **C, D:** Percentage of glomerular and tubulointerstitial collagen I accumulation. **E, F:** Percentage of glomerular and tubulointerstitial collagen III deposition. Each **bar** represents data (mean ± SEM) for groups of six rats treated with Smad7 (**hatched bars**), empty vector (**filled bars**), or normal sham-controls (**open bars**). *, $P < 0.05$; **, $P < 0.01$; and ***, $P < 0.001$, when compared to empty vector-treated controls; [b], $P < 0.01$ and [c], $P < 0.001$, when compared to normal sham-control.

α-SMA and collagen matrix accumulation in sham, control vector-treated, and Smad7-treated animals were assessed by one-way analysis of variance, followed by *t*-test.

Results

Ultrasound-Mediated Gene Transfer of Inducible Smad7 Attenuates Progressive Renal Functional and Histological Injury Independent of Blood Pressure in Remnant Kidney Disease

After subtotal nephrectomy, hypertension developed in both Smad7- and empty vector-treated rats. Blood pressure was significantly elevated at the end of the first week after nephrectomy compared to sham-operated animals ($P < 0.001$), and the rise in blood pressure was equivalent (systolic blood pressure 190 to 200 mmHg) in both Smad7-treated animals and empty vector-treated controls (Figure 1A). Nephrectomized rats that were treated with empty vector developed progressive renal injury as evidenced by the significant increase in 24-hour proteinuria (Figure 1B) and serum creatinine (Figure 1C), and the decline in creatinine clearance (Figure 1D). In contrast, Smad7 gene therapy blunted the rise in proteinuria and serum creatinine (Figure 1, B and C; $P < 0.001$), and prevented the fall in creatinine clearance after 5/6 nephrectomy (Figure 1D; $P < 0.001$). Histologically, there were no obvious pathological changes such as focal and

segmental glomerulosclerosis in both empty vector-treated or Smad7-treated animals (Figure 2). However, compared to the normal sham-control kidney (Figure 2A), diseased kidney in empty vector-treated animals developed severe tubulointerstitial damage as evidenced by the development of tubular atrophy and dilatation, the presence of numerous protein casts, and the emergence of interstitial fibrosis. Strikingly, empty vector-treated animals displayed vascular intimal hyperplasia, medial hypertrophy, and severe arterial sclerosis (Figure 2B). In contrast, treatment with Smad7 preserved renal histology and prevented the vascular and tubulointerstitial damage that follows 5/6 nephrectomy (Figure 2C).

Inhibition of ECM Expression Is a Central Mechanism by which Gene Transfer of Smad7 Prevents Progressive Renal Injury in Rat Remnant Kidney Disease

Next, we investigated the potential mechanisms whereby gene therapy with Smad7 inhibits progressive renal injury in a rat remnant kidney disease. The suppressive effects of doxycycline-induced Smad7 expression on renal fibrosis were quantitated by measuring α-SMA, collagen type I, and collagen type III mRNA and protein expression by real time-PCR, Western blotting, and immunohistochemistry. As shown in Figure 3, quantitative real-time PCR demonstrated that renal α-SMA and collagen I and III mRNA expression were markedly up-regulated in empty vector-treated animals, whereas overexpression of Smad7 in the remnant kidney (Figure 3A) resulted in substantial inhibition of α-SMA (Figure 3B) and collagen type I and III (Figure 3, C and D) mRNA expression. Western blot analysis of α-SMA, collagen I, and collagen III proteins also demonstrated that, overexpression of Smad7 in the remnant kidney produced a marked inhibition of α-SMA and collagen I and III protein expression, compared to empty vector-treated controls (Figure 4). Furthermore, immunohistochemistry showed that, compared to kidneys of sham-operated controls, remnant kidneys of empty vector-treated rats exhibited severe tubulointerstitial fibrosis as evidenced by prominent α-SMA+ cell staining and collagen type I and III deposition, which were substantially inhibited by gene therapy with Smad7 (Figure 5). Semiquantitative analysis of immunohistochemistry using a quantitative Image Analysis System revealed that Smad7 gene therapy significantly inhibited α-SMA, collagen I and III accumulation in both glomeruli and tubulointerstitium (Figure 6).

TGF-β/Smad Signaling Is the Key Pathway for Renal Fibrosis in Hypertensive Nephropathy and Blockade of Smad2/3 Activation Is a Key Mechanism by which Overexpression of Smad7 Prevents Renal Fibrosis

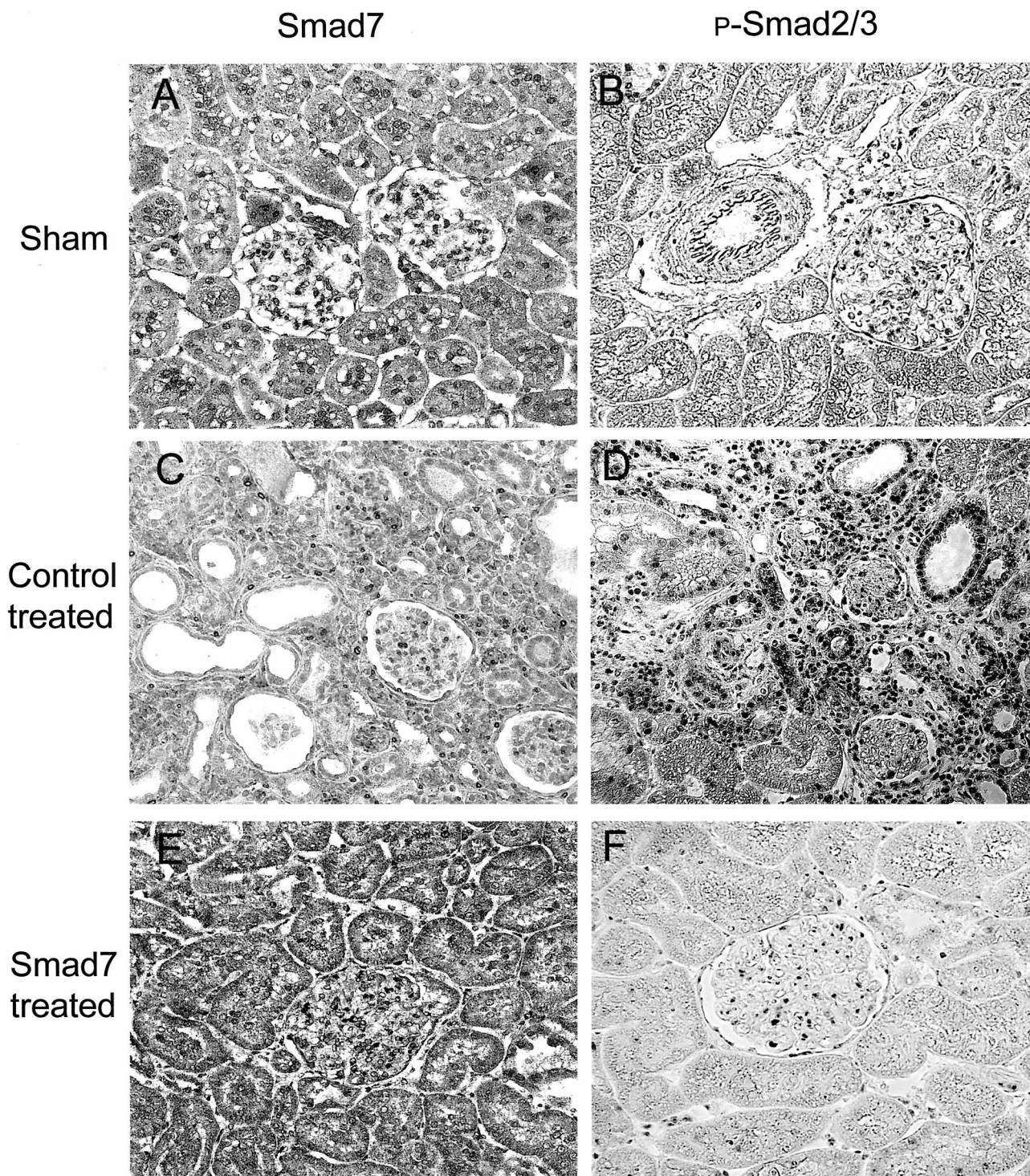It is now well established that TGF-β stimulates ECM production via Smad signaling pathway. We tested whether

Smad7   P-Smad2/3

Figure 7. Immunohistochemistry demonstrates that overexpression of Smad7 inhibits phosphorylated Smad2/3 nuclear translocation within the kidney. A, B: Normal sham-control. C, D: Empty vector treatment. E, F: Smad7 treatment. Results show that compared to the normal sham-control (A, B), expression of Smad7 is slightly decreased in empty vector-treated rats (C) and this is associated with a marked increase in p-Smad2/3 nuclear location (D). In contrast, overexpression of Smad7 (E) results in substantial inhibition of p-Smad2/3 activation (F). Original magnifications, ×100.

inhibition of Smad2/3 activation is a central mechanism whereby overexpression of Smad7 prevents renal fibrosis in rat remnant kidney disease. As shown in Figures 7 and 8, Smad7 was constitutively expressed in both glomeruli and tubulointerstitial cells in the normal sham-control kidney (Figure 7A), and there were few cells with positive

nuclear staining for Smad2/3 (Figure 7B). On the other hand, remnant kidneys of empty vector-treated animals showed reduction of Smad7 expression; and this was associated with strong activation of Smad2/3 in tubulointerstitial cells and the development of severe tubulointerstitial fibrosis (Figure 7, C and D). However, activation of
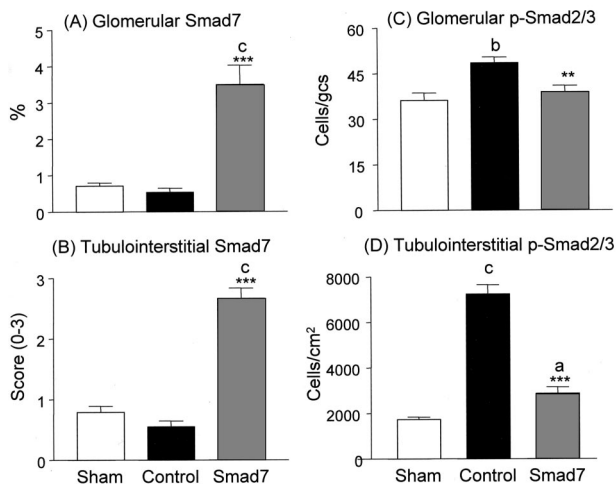
Figure 8. Semiquantitative analysis of the therapeutic effect of Smad7 on phosphorylated Smad2/3 nuclear localization in the glomerulus and tubulointerstitium using the Quantitative Image System. **A, B:** Degree of glomerular and tubulointerstitial Smad7 expression. **C, D:** Numbers of glomerular and tubulointerstitial cells with nuclear localization of p-Smad2/3. Each **bar** represents data (mean ± SEM) for groups of six rats treated with Smad7 (**hatched bars**), empty vector (**filled bars**), or normal sham-control (**open bars**). **, $P < 0.01$ and ***, $P < 0.001$, when compared to empty vector-treated controls; [b], $P < 0.01$ and [c], $P < 0.001$, when compared to the normal sham-control.

Figure 9. Western blot and immunoprecipitation analyses show the inhibitory effect of Smad7 gene transfer on renal Smad2/3 phosphorylation. Smad7 is detected by Western blot, whereas Smad2/3 phosphorylation is determined by immunoprecipitation as described in the Materials and Methods. Compared to normal sham-controls, Smad7 expression is slightly reduced in empty vector-treated animals, whereas overexpression of Smad7 substantially inhibits Smad2/3 phosphorylation. Each **lane** represents one rat kidney and each **bar** represents semiquantitative data (mean ± SEM) for groups of six rats treated with Smad7 (**hatched bars**), empty vector (**filled bars**), or normal sham-control (**open bars**). *, $P < 0.05$ and **, $P < 0.01$, when compared to empty vector-treated controls; [b], $P < 0.01$ and [c], $P < 0.001$, when compared to the normal sham-control.

Smad2/3 in the glomeruli was less apparent (Figures 7 and 8), and was accompanied by mild glomerular fibrosis (Figures 5 and 6). In contrast, Smad7-treated rats showed significantly higher level of Smad7 expression in cells of both glomeruli and tubulointerstitium (Figure 7E), which was associated with substantial inhibition of Smad2/3 activation and prevention of kidney damage (Figure 7F). Semiquantitative analysis for Smad7 expression and Smad2/3 activation (nuclear translocation of phosphorylated Smad2/3) revealed that overexpression of Smad7 was coupled with substantial inhibition of Smad2/3 activation in the diseased kidney (Figure 8). This was further confirmed by Western blot analysis of phosphorylated Smad2/3 in which overexpression of Smad7 in the remnant kidney, using gene transfer, decreased the level of activated (phosphorylated) Smad2/3, in comparison with empty vector-treated controls (Figure 9).

Overexpression of Smad7 Prevents Severe Vascular Damage in Rat Remnant Kidney Disease

One striking picture in rat remnant kidney disease was the development of severe vascular damage including proliferative vasculopathy and arteriolosclerosis (Figure 2B). Proliferative and sclerotic vascular lesions were evident in all animals treated with control empty vectors, consisting of 40 to 60% of arteries examined in the entire cortical cross-section. In contrast, no vascular lesions were found in the entire cortex in those treated with Smad7. As shown in Figures 10 and 11, the development of severe vascular sclerosis as demonstrated by massive collagen matrix accumulation (Figures 10D and 11B) was associated with marked activation of vascular Smad2/3
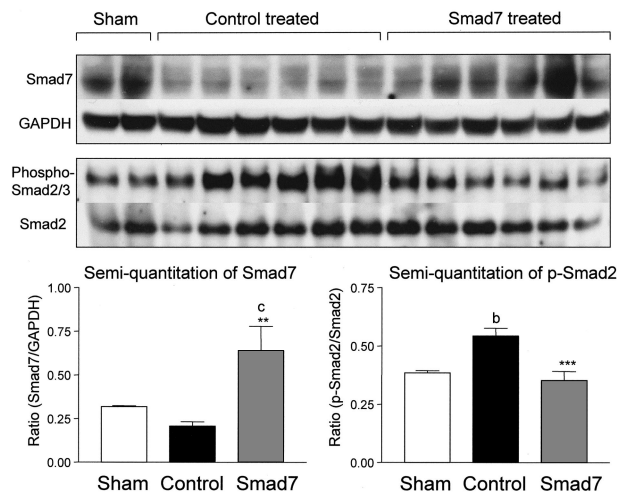
(Figures 10C and 11A) in the remnant kidney treated with control vectors. In contrast, gene transfer with Smad7 completely prevented the vascular Smad2/3 activation (Figures 10E and 11C) and arteriolosclerosis including collagen matrix accumulation within the arterial walls although collagen accumulation in the perivascular area remained evident (Figures 10F and 11D).

Discussion

This study demonstrates that gene transfer of inducible Smad7 can attenuate fibrosis in rat remnant kidney disease. Activation of TGF-β/Smad signaling is a key pathway leading to progressive renal scaring in association with hypertension. Blockade of Smad2/3 activation is a central mechanism by which overexpression of Smad7 inhibits renal fibrosis including α-SMA, collagen type I, and collagen type III expression. Furthermore, the ability of gene transfer of inducible Smad7 to block TGF-β/Smad signaling and renal fibrosis in rat remnant kidney also demonstrates that ultrasound-microbubble-mediated Smad7 gene therapy may have therapeutic potential for treatment of kidney disease in association with hypertension.

Increasing evidence has shown that Ang II plays a major role in renal fibrosis in hypertensive and diabetic kidney diseases.[1–6,12–16] The induction of TGF-β by Ang II is considered as a central mechanism of hypertensive nephropathy,[4,5,12–16] and inhibition of TGF-β production by Ang II receptor blockers or angiotensin-converting enzyme inhibitors may underlie the renoprotective effect of these agents in patients with diabetes and hypertension. The recent discovery and characterization of TGF-β/Smad signaling has allowed better understanding of
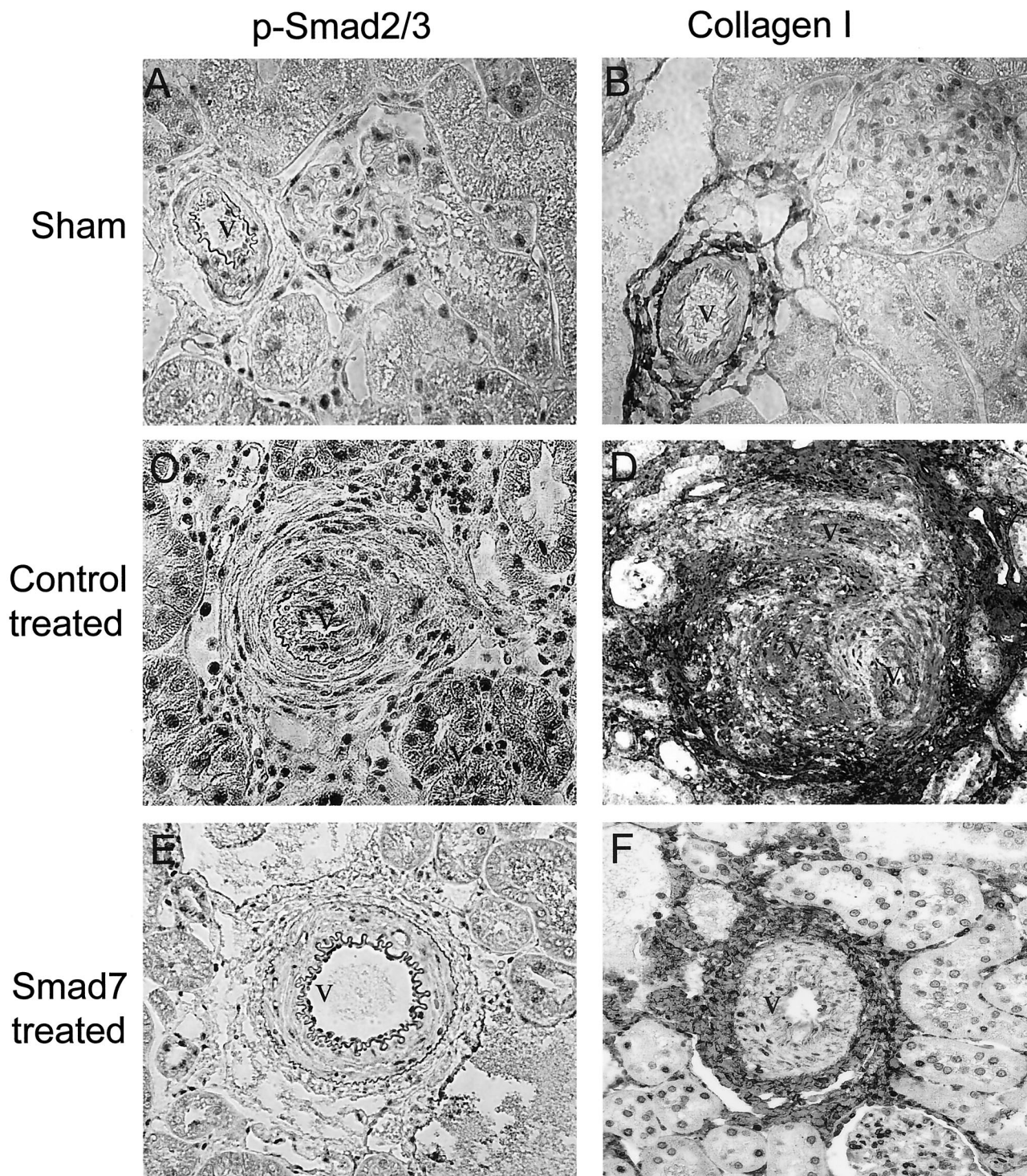
p-Smad2/3   Collagen I

Figure 10. Immunohistochemistry demonstrates that gene therapy with Smad7 inhibits Smad2/3 activation and vascular sclerosis. **A, B:** Sham-operating kidneys. Vascular Smad2/3 activation as determined by nuclear translocation of phosphorylated Smad2/3 (**A**) and collagen expression in arterial (v) and periarterial areas. **C, D:** Empty vector-treated remnant kidneys. **E, F:** Smad7-treated remnant kidneys. Results show that marked activation of vascular p-Smad2/3 is associated with the development of severe vascular sclerosis as demonstrated by strong collagen matrix accumulation (v) in the kidney treated with control empty vector (**C, D**), which is completely blocked by Smad7 treatment (**E, F**). Original magnifications, ×200.

the pathogenesis of fibrosis and identified Smad7 as a potential target for anti-fibrosis therapy. We and other investigators have shown that gene transfer of Smad7 prevents renal fibrosis in a rat model of obstructive kidney disease,[31,32] as well as in other fibrotic disease models

such as bleomycin-induced pulmonary fibrosis[35] and liver fibrosis after bile duct obstruction.[36] However, it remains unknown whether blockade of TGF-β/Smad signaling inhibits renal disease in association with hypertension. The present study provides the first evidence that
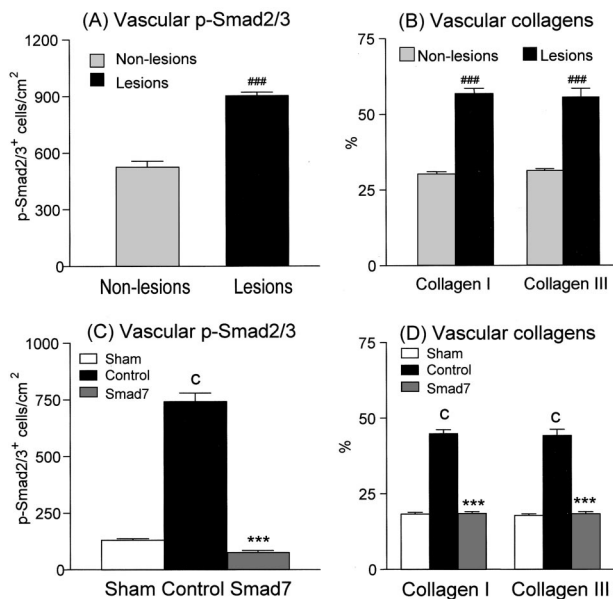
Figure 11. Semiquantitative analysis of the therapeutic effect of Smad7 on vascular phosphorylated Smad2/3 nuclear localization and arteriolosclerosis. **A, B:** Smad2/3 activation and collagen I and collagen III accumulation in vascular areas with (**solid bars**) or without (**dotted bars**) the development of arterial sclerotic lesions in empty vector-treated remnant kidney. **C, D:** Effect of Smad7 treatment on vascular Smad2/3 activation and arteriolosclerosis. Vascular p-Smad2/3 and collagen matrix accumulation is markedly increased in empty vector-treated rats, resulting in severe vascular damage (**A, B**), which is prevented by Smad7 treatment (**C, D**). Data shown in **A** and **B** were obtained from the arterial walls and periarterial regions with proliferative and sclerotic vasculopathy (lesions) or without vascular damage (non-lesions) in empty vector-treated rat remnant kidneys ($n = 6$) as described in the Materials and Methods. Each **bar** represents data (mean ± SEM) for groups of six rats treated with Smad7 (**hatched bars**), empty vector (**filled bars**), or normal sham-control (**open bars**). ###, $P < 0.001$, when compared to those without proliferative/sclerotic vascular lesions (**A, B**); ***, $P < 0.001$, when compared to empty vector-treated controls (**C, D**); and c, $P < 0.001$, when compared to the normal sham-control (**C, D**).

overexpression of Smad7 can block the TGF-β/Smad signaling pathway and prevent renal fibrosis in 5/6 nephrectomized rat model, a kidney disease with hypertension. The ability of Smad7 overexpression to block Smad2/3 activation and renal fibrosis as evidenced by the substantial reduction in α-SMA, collagen I, and collagen III expression strongly suggests that TGF-β/Smad signaling plays a critical role in the pathogenesis of progressive renal injury in hypertension.

A novel and important observation in this study is that overexpression of Smad7 can inhibit arteriolosclerosis without lowering blood pressure. This observation indicates that blood pressure may stimulate Smad signaling independent of TGF-β by renin-angiotensin system and causes vascular damage and hypertensive kidney disease. Thus, Smad signaling may represent a central pathway leading to hypertensive kidney disease regardless of whether the hypertension is caused by activation of renin-angiotensin-system or by other mechanisms.

A central role for Smad signaling in diabetic nephropathy has been reported.[28] Although high glucose stimulates renal tubular, mesangial, endothelial, and vascular smooth muscle cells to produce ECM via a TGF-β-dependent Smad signaling mechanism,[37] recent data suggest that advanced glycation end products activate

Smad2/3 and induce ECM production via TGF-β-dependent and/or -independent mechanisms;[28] the latter appears to involve ERK and p38 MAP kinase.[28,34] It may be possible that Ang II as well as high blood pressure can activate Smad signaling via both TGF-β-dependent and -independent mechanisms, which require further investigations.

The renoprotective effect of ultrasound-microbubble-mediated inducible Smad7 gene therapy on progressive renal injury in 5/6 nephrectomized rat model is significant and relevant clinically. It indicates that this gene delivery system may be a new therapeutic strategy for hypertensive kidney disease including diabetic nephropathy. As shown in our previous study in rat obstructive kidney, the ultrasound-microbubble-mediated system is a safe and highly effective gene therapy technique. Our data demonstrated the feasibility of effective transfection of Smad7 gene in the kidney to more than 90% of glomerular, tubular, and interstitial cells including vascular cells, and the ability to tightly regulate Smad7 transgene expression at therapeutic levels without notable renal toxicity.[31]

In summary, we have demonstrated that gene transfer of inducible Smad7 using the ultrasound-microbubble-mediated system can attenuate renal fibrosis in the hypertensive rat remnant kidney model. Transfer of inducible Smad7 gene into the kidney provides a powerful tool for the treatment of chronic kidney disease, and reinforces findings by previous studies that support the utility, safety, and effectiveness of ultrasound-microbubble-mediated gene transfer for therapeutic purposes.

References

1. Flack JM, Peters R, Shafi T, Alrefai H, Nasser SA, Crook E: Prevention of hypertension and its complications: theoretical basis and guidelines for treatment. J Am Soc Nephrol 2003, 14(Suppl 2):S92–S98
2. Klahr S, Morrissey J: Progression of chronic renal disease. Am J Kidney Dis 2003, 41(Suppl 1):S3–S7
3. Taal MW, Brenner BM: Renoprotective benefits of RAS inhibition: from ACEI to angiotensin II antagonists. Kidney Int 2000, 57:1803–1817
4. Border WA, Noble NA: Interactions of transforming growth factor-beta and angiotensin II in renal fibrosis. Hypertension 1998, 31:181–188
5. Gaedeke J, Peters H, Noble NA, Border WA: Angiotensin II, TGF-beta and renal fibrosis. Contrib Nephrol 2001, 135:153–160
6. Wolf G: Link between angiotensin II and TGF-beta in the kidney. Miner Electrolyte Metab 1998, 24:174–180
7. Wolf G, Haberstroh U, Neilson EG: Angiotensin II stimulates the proliferation and biosynthesis of type I collagen in cultured murine mesangial cells. Am J Pathol 1992, 140:95–107
8. Kagami S, Border WA, Miller DE, Noble NA: Angiotensin II stimulates extracellular matrix protein synthesis through induction of transforming growth factor-beta expression in rat glomerular mesangial cells. J Clin Invest 1994, 93:2431–2437
9. Wolf G, Zahner G, Schroeder R, Stahl RA: Transforming growth factor beta mediates the angiotensin-II-induced stimulation of collagen type IV synthesis in cultured murine proximal tubular cells. Nephrol Dial Transplant 1996, 11:263–269
10. Wolf G, Ziyadeh FN, Stahl RA: Angiotensin II stimulates expression of transforming growth factor beta receptor type II in cultured mouse proximal tubular cells. J Mol Med 1999, 77:556–564
11. Gibbons GH, Pratt RE, Dzau VJ: Vascular smooth muscle cell hypertrophy vs hyperplasia: autocrine transforming growth factor-beta 1 expression determines growth response to angiotensin II. J Clin Invest 1992, 90:456-461
12. Rumble JR, Gilbert RE, Cox A, Wu L, Cooper ME: Angiotensin converting enzyme inhibition reduces the expression of transforming

growth factor-beta(1) and type IV collagen in diabetic vasculopathy. J Hypertens 1998, 16:1603-1609

13. Peters H, Border WA, Noble NA: Targeting TGF-beta overexpression in renal disease: maximizing the antifibrotic action of angiotensin II blockade. Kidney Int 1998, 54:1570–1580

14. Benigni A, Zoja C, Corna D, Zatelli C, Conti S, Campana M, Gagliardini E, Rottoli D, Zanchi C, Abbate M, Ledbetter S, Remuzzi G: Add-on anti-TGF-beta antibody to ACE inhibitor arrests progressive diabetic nephropathy in the rat. J Am Soc Nephrol 2003, 14:1816–1824

15. Houlihan CA, Akdeniz A, Tsalamandris C, Cooper ME, Jerums G, Gilbert RE: Urinary transforming growth factor-beta excretion in patients with hypertension, type 2 diabetes, and elevated albumin excretion rate: effects of angiotensin receptor blockade and sodium restriction. Diabetes Care 2002, 25:1072–1077

16. Agarwal R, Siva S, Dunn SR, Sharma K: Add-on angiotensin II receptor blockade lowers urinary transforming growth factor-beta levels. Am J Kidney Dis 2002, 39:486–492

17. Isaka Y, Fujiwara Y, Ueda N, Kaneda Y, Kamada T, Imai E: Glomerulosclerosis induced by in vivo transfection of transforming growth factor-β or platelet-derived growth factor gene into the rat kidney. J Clin Invest 1993, 92:597–601

18. Akagi Y, Isaka Y, Arai M, Kaneko T, Takenaka M, Moriyama T, Kaneda Y, Ando A, Orita Y, Kamada T, Ueda N, Imai E: Inhibition of TGF-β 1 expression by antisense oligonucleotides suppressed extracellular matrix accumulation in experimental glomerulonephritis. Kidney Int 1996, 50:148–155

19. Isaka Y, Brees DK, Ikegaya K, Kaneda Y, Imai E, Noble NA, Border WA: Gene therapy by skeletal muscle expression of decorin prevents fibrotic disease in rat kidney. Nat Med 1996, 2:418–423

20. Ziyadeh FN: Mediators of diabetic renal disease: the case for TGF-beta as the major mediator. J Am Soc Nephrol 2004, 15(Suppl 1):S55–S57

21. Kretzschmar M, Massague J: Smads: mediators and regulators of TGF-β signaling. Curr Opin Genet Dev 1998, 8:103–111

22. Kavsak P, Rasmussen RK, Causing CG, Bonni S, Zhu H, Thomsen GH, Wrana JL: Smad7 binds to Smurf2 to form an E3 ubiquitin ligase that targets the TGF-β receptor for degradation. Mol Cell 2000, 6:1365–1375

23. Poncelet AC, Schnaper HW: Sp1 and Smad proteins cooperate to mediate transforming growth factor-β 1-induced α 2(I) collagen expression in human glomerular mesangial cells. J Biol Chem 2001, 276:6983–6992

24. Schnaper HW, Hayashida T, Poncelet AC: It's a Smad world: regulation of TGF-beta signaling in the kidney. J Am Soc Nephrol 2002, 13:1126–1128

25. Bottinger EP, Bitzer M: TGF-β1 signaling in renal disease: J Am Soc Nephrol 2002, 13:2600–2610

26. Schiffer M, Schiffer LE, Gupta A, Shaw AS, Roberts IS, Mundel P, Bottinger EP: Inhibitory Smads and TGF-beta signaling in glomerular cells. J Am Soc Nephrol 2002, 13:2657–2666

27. Isono M, Chen S, Hong SW, Iglesias-de la Cruz MC, Ziyadeh FN: Smad pathway is activated in the diabetic mouse kidney and Smad3 mediates TGF-beta-induced fibronectin in mesangial cells. Biochem Biophys Res Commun 2002, 296:1356–1365

28. Li JH, Huang XR, Zhu HJ, Oldfield M, Cooper M, Truong LD, Johnson RJ, Lan HY: Advanced glycation end products activate Smad signaling via TGF-beta-dependent and independent mechanisms: implications for diabetic renal and vascular disease. FASEB J 2004, 18:176–178

29. Li JH, Zhu HJ, Huang XR, Lai KN, Johnson RJ, Lan HY: Smad7 inhibits fibrotic effect of TGF-β on renal tubular epithelial cells by blocking Smad2 activation. J Am Soc Nephrol 2002, 13:1464–1472

30. Chen R, Huang C, Morinelli TA, Trojanowska M, Paul RV: Blockade of the effects of TGF-β1 on mesangial cells by overexpression of Smad7. J Am Soc Nephrol 2002, 13:887–893

31. Lan HY, Mu W, Tomita N, Huang XR, Li JH, Zhu HJ, Morishita R, Johnson RJ: Inhibition of renal fibrosis by gene transfer of inducible Smad7 using ultrasound-microbubble system in rat UUO model. J Am Soc Nephrol 2002, 14:1535–1548

32. Terada Y, Hanada S, Nakao A, Kuwahara M, Sasaki S, Marumo F: Gene transfer of Smad7 using electroporation of adenovirus prevents renal fibrosis in post-obstructed kidney. Kidney Int 2002, 61:S94–S98

33. Ng YY, Huang TP, Yang WC, Chen ZP, Yang AH, Mu W, Nikolic-Paterson DJ, Atkins RC, Lan HY: Tubular epithelial-myofibroblast transdifferentiation in progressive tubulointerstitial fibrosis in 5/6 nephrectomized rats. Kidney Int 1998, 54:864–876

34. Li JH, Wang W, Huang XR, Oldfield M, Schmidt AM, Cooper ME, Lan HY: Advanced glycation end products induce tubular epithelial-myofibroblast transition through the RAGE-ERK1/2 MAP kinase signaling pathway. Am J Pathol 2004, 164:1389–1397

35. Nakao A, Fujii M, Matsumura R, Kumano K, Saito Y, Miyazono K, Iwamoto I: Transient gene transfer and expression of Smad7 prevents bleomycin-induced lung fibrosis in mice. J Clin Invest 1999, 104:5–11

36. Dooley S, Hamzavi J, Breitkopf K, Wiercinska E, Said HM, Lorenzen J, Ten Dijke P, Gressner AM: Smad7 prevents activation of hepatic stellate cells and liver fibrosis in rats. Gastroenterology 2003, 125:178–191

37. Li JH, Huang XR, Zhu HJ, Johnson R, Lan HY: Role of TGF-beta signaling in extracellular matrix production under high glucose conditions. Kidney Int 2003, 63:2010–2019